ESKİŞEHİR TECHNICAL UNIVERSITY JOURNAL OF SCIENCE AND TECHNOLOGY
A- APPLIED SCIENCES AND ENGINEERING

2020, 21(4), pp. 562-574, DOI: 10.18038/estubtda.622914

RESEARCH ARTICLE

PHYSICAL AND MECHANICAL CHARACTERISATION OF ASBESTOS-FREE PARTICULATE CERAMIC MATRIX COMPOSITES

Olatunde SEKUNOWO [1], Stephen DUROWAYE [1,*], Ganiyu LAWAL [1]

[1] Metallurgical and Materials Engineering Department, University of Lagos, Nigeria

ABSTRACT

Production of friction particulate ceramic matrix composites (PCMCs) by powder metallurgy method was carried out using iron 105 µm millscale, 50 µm silica sand, 80 µm magnesia and 53 µm bentonite clay as input materials. Different formulation of the blend of these materials were prepared and the composites were produced. Microstructural, water absorption, and mechanical characterisation were determined using standardised methods. The ceramic composites exhibited very good properties in terms of density, water absorption, hardness, compressive strength, shear strength and impact energy. The specific values of these properties exhibited by sample D in terms of density (1.87 g/cm^3), water absorption (0.3 %) indicating reduced pores/voids, hardness (147.09 BHN), compressive strength (156.45 MPa), shear strength (5.97 MPa) and impact energy (7.62 J) are desirable. The uniform dispersion of the particles as observed in the microstructure and strong bonding/adhesion contributed to the enhancement of the properties. These results compared favourably well with that of conventional automobiles brake pads which is an indication that the composites are very suitable for application as automobiles brake pads.

Keywords: Particulate ceramic matrix composites, Powder metallurgy, Microstructure, Physical properties, Mechanical properties

1. INTRODUCTION

The development and application of automobiles brake pads are dated back to over ten decades ago. Asbestos, metals, ceramics and organic materials are usually the major components of brake pads. Asbestos is a human carcinogen which causes cancer. Due to the detrimental effect of asbestos to the human health, its use has been highly restricted or baned in many parts of the world. This has led to the development of asbestos-free brake pads.

Brake pads are vital components of the brake system of automobiles. They are fixed to steel backing plates with the pads facing the brake disc. When the brake is applied, the pads are forced outward and pressed against the discs to effect speed reduction or stoppage of vehicles.

Brake pads are usually tested to ascertain the characteristics or properties that make them to be suitable for the intended application. Composite brake pads are frequently tested for mechanical properties before friction and wear testing. Amongst the major parameters to be determined usually include hardness, toughness, specific gravity, compressive strength, shear strength, oil absorption and water absorption [1]. For effective/optimal performance, brake pads should have low moisture sensitivity, low shrinkage, adequate mechanical strength, good bonding to the backing plate among other properties [2].

Safety and comfort are the two major sought-after values by operators and passengers in automobiles. However, safety is often threatened when brake pads of automobiles are made from low quality materials which do not exhibit the desirable mechanical properties, thermal stability and wear resistance. One of the reasons why automobiles brakes experience failure is due to the heat generated during braking causing adiabatic heating of the brake pads which reduces braking efficiency. Accumulated heat within the brake system usually causes gradual thermal expansion and composition debonding of the brake

---

*Corresponding Author: durosteve02@yahoo.com
Received: 20.09.2019 Published: 28.12.2020

pads resulting in impaired structural integrity and loss of friction. Further, these conditions aggravate the rate of wear of the brake pads surfaces which reduces its arresting capability resulting in brake-failure. The combination of these dysfunctional occurrences usually have adverse effect on brake pads in terms of performance and durability. Hence, the need to develop materials that will exhibit desirable physical, mechanical, thermal and tribological properties.

In an attempt to solve these problems, different materials have been used to develop brake pads. Among the materials used are: maize husks – MH [3], cocoa beans shells – CBS [4], palm kernel shells – PKS [5] etc. These materials have some characteristics that make them qualify as potential materials for use in the development of brake pads [6, 7, 8]. Composite brake pads have been successfully used in automobiles as replacement for asbestos brake pads. This is as a result of the desirable physical, mechanical, thermal and tribological properties which they exhibit. Composites are multiple phase materials produced through combination of different materials in order to obtain properties that the individual components do not possess. The complexity of brake systems is the reason why brake pads are no longer composed of monolithic materials. Composite friction materials can be moulded into shaped linings, friction blocks, and pads depending on the brake system in use. The effectiveness of the brakes depends to a large extent on the quality and composition of the brake pads [9, 10].

The use of locally available materials for production of brake pads for automobiles use is being encouraged because some of these materials possess desirable functional properties coupled with environmental friendliness, and their use can also subsidize price. This work is aimed at producing a friction composite material by powder metallurgy method using locally available materials such as iron millscale, silica sand, magnesia and bentonite clay for application as automobiles brake pad taking into consideration cost, durability and environmental implication.

2. EXPERIMENTAL

2.1. Materials

Iron millscale, silica sand, magnesia, and bentonite are the materials used and were all obtained in Nigeria. The photographs of these materials and their chemical composition determined by X-ray fluorescence are shown in Figure 1 and Table 1 respectively.

Figure 1. Photographs of input materials (a) 105 μm iron millscale particles, (b) 53 μm bentonite clay particles, (c) 80 μm magnesia particles, (d) 50 μm silica sand particles.

Table 1. Composition of the input materials by weight percent

Compounds	**Amount (wt. %)**			
	Iron Millscale	**Silica**	**Magnesia**	**Bentonite**
FeO	69.57	0.04	-	-
Fe_2O_3	24.08	0.16	-	3.89
Fe_3O_4	6.06	0.001	-	-
SiO_2	0.02	99.52	0.01	63.57
MgO	0.03	0.02	99.94	2.64
CaO	0.19	0.03	0.02	1.33
MnO	0.03	0.02	-	-
Al_2O_3	0.02	0.19	-	25.63
Na_2O	-	0.006	-	2.31
K_2O	-	0.004	-	0.51
TiO_2	-	-	-	0.12
L.O.I	-	0.001	0.03	-

L.O.I = Loss on ignition

2.2. Composite Samples Production

The as-received silica sand and iron millscale were ground by using a pulverizer and manually sieved to 50 μm and 105 μm particle sizes respectively using British standard sieves (BSS). These materials were manually blended with 80 μm magnesia and 53 μm bentonite according to the formulation presented in Table 2 to obtained many formulations of samples A, B, C, D and E. Appropriate quantity of water was added to each blend. Thereafter, each of the wet-mixed blends was poured into the fabricated metallic mould and compacted at 0.33 MPa using a presser. An engine oil (Mobil XHP) was applied on the inner part of the mould to facilitate an easy removal of the of the samples from the mould. The samples were sun dried (30-32^0 C) for 24 hours in an oven at 110^0 C for 24 hours to ensure complete removal of water from the samples. A muffle furnace pre-set at heating rate of 10^0 C/min was used to sinter the samples at 1200^0 C. After 3 hours of sintering, the samples were removed and cooled at room temperature. This is to enhance bonding of the particles for properties enhancement. This production process is similar to the one employed by [11]. The photographs of some of the composite samples and brake pads produced are shown in Figure 2.

Table 2. Materials formulation in weight percent (wt. %)

Sample	**Iron millscale (wt. %)**	**Silica (wt. %)**	**Magnesia (wt. %)**	**Bentonite (wt. %)**	**Total (wt. %)**
A	0	5	15	80	100
B	4	5	15	76	100
C	8	5	15	72	100
D	12	5	15	68	100
E	16	5	15	64	100

Figure 2a. Photograph of some of the composite samples produced.

Figure 2b. Photograph of some of the composite samples produced.

Figure 2c. Photograph of two samples of composite brake pads produced.

2.3. Properties Characterisation

The microstructural examination of the samples was done with the aid of a scanning electron microscope (SEM). Archimedes' principle was used to determine the density of the samples at room temperature. The mass of the samples in air was measured and then submerged in water. Their densities were then determined based on buoyancy of water using Equation 1 which was earlier adopted by [4, 11].

$$\text{Density } (\rho) = \frac{\text{Mass (g)}}{\text{Volume (cm)}^3} \qquad 1$$

To determine the water absorption of the samples, their initial weight (W_1) was measured after which they were submerged in water in a beaker and reweighed (W_2) after soaking in water for two days. The water absorption (W_A) of the composite was determined in accordance with ISO 175:1999 (E) standard using Equation 2 which was also earlier adopted by [12, 13].

$$W_A(\%) = \frac{W_2 - W_1}{W_1} \text{ x } 100 \tag{2}$$

Determination of the samples' hardness was carried out in accordance with ASTM E10 standard. The compressive strength of the samples was determined according to ASTM D695 standard using an Instron universal tester. The shear strength of the samples was also determined according to ASTM D7078 standard using the same Instron universal tester while an Izod impact tester was used to determine the impact energy according ASTM D256 standard.

3. RESULTS AND DISCUSSION

3.1. Microstructure of the Samples

As presented in Figures 3 – 7, the micrographs revealed that there was inhomogeneity in the microstructure of the samples as particles appeared in dendritic and oval shapes while the energy-dispersive X-ray spectroscopy (EDS) spectra revealed the elemental composition of the samples. There was presence of O, Si, Al, Mg and Ca in sample A while samples B, C, D and E also contained these elements and Fe (iron) inclusive. Some of the EDS spectra also revealed that there were some phases that could not be distinguished which indicated that other elements were present in traces. The whitish spots in the microstructure were likely MgO phase from the magnesia while the dark spots were likely FeO phase from the millscale. The ash coloured needle-like portions were likely the mullite ($3Al_2O_3 \cdot 2SiO_2$) phases which is a highly crystalline ceramic compound from bentonite-silica mixture and the gray mixed with whitish spots are likely the spinel phase formed during sintering of the samples. The micrographs in Figures 4 – 7 showed that the FeO was well dispersed in the microstructure with no obvious agglomeration. Microstructures also showed good adhesion of the particles as a result of sintering between the millscale particles and the matrix particles is observed.

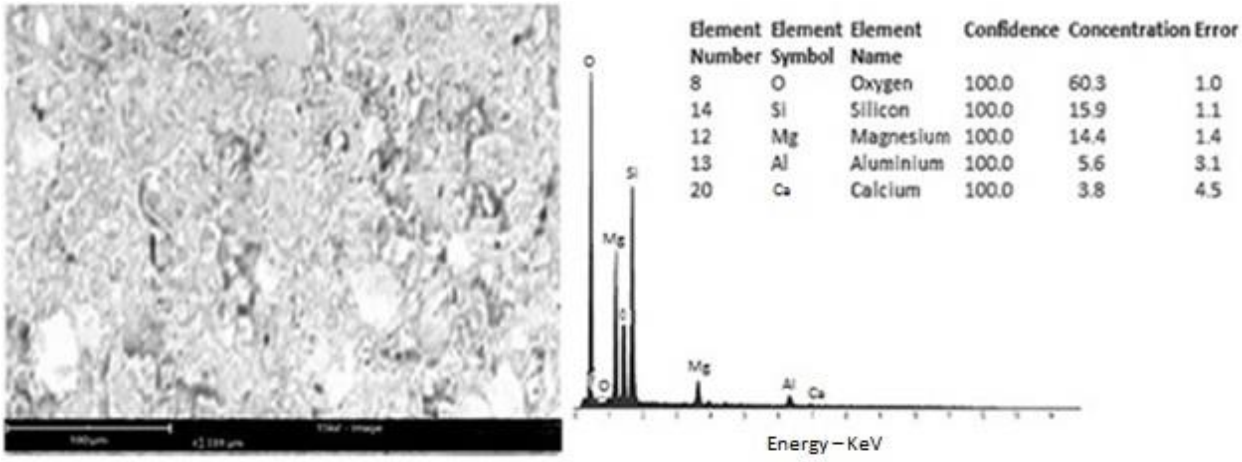

Element Number	Element Symbol	Element Name	Confidence	Concentration	Error
8	O	Oxygen	100.0	60.3	1.0
14	Si	Silicon	100.0	15.9	1.1
12	Mg	Magnesium	100.0	14.4	1.4
13	Al	Aluminium	100.0	5.6	3.1
20	Ca	Calcium	100.0	3.8	4.5

Figure 3. Micrograph and EDS spectrum of composite sample A.

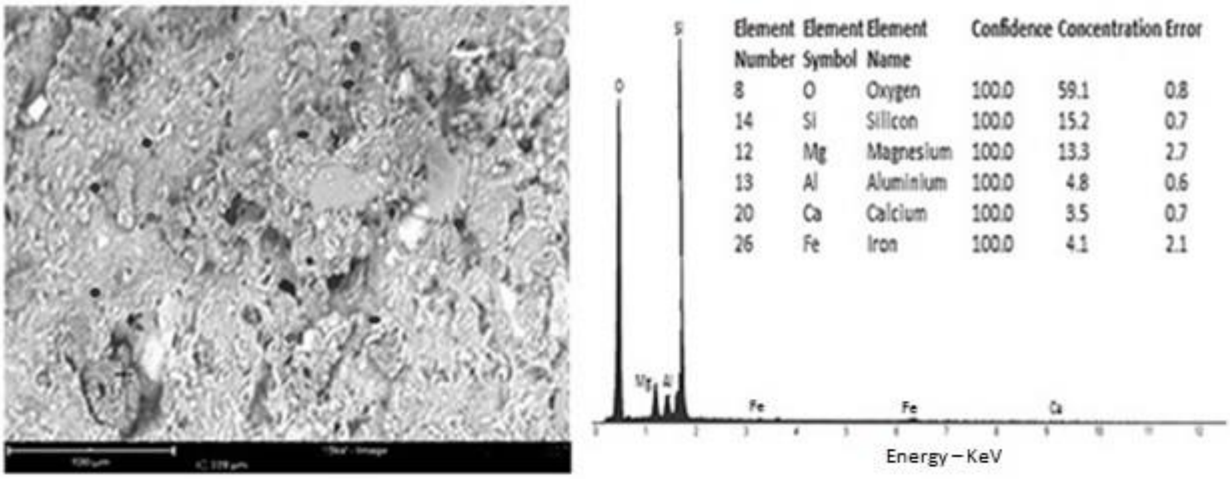

Element Number	Element Symbol	Element Name	Confidence	Concentration	Error
8	O	Oxygen	100.0	59.1	0.8
14	Si	Silicon	100.0	15.2	0.7
12	Mg	Magnesium	100.0	13.3	2.7
13	Al	Aluminium	100.0	4.8	0.6
20	Ca	Calcium	100.0	3.5	0.7
26	Fe	Iron	100.0	4.1	2.1

Figure 4. Micrograph and EDS spectrum of composite sample B.

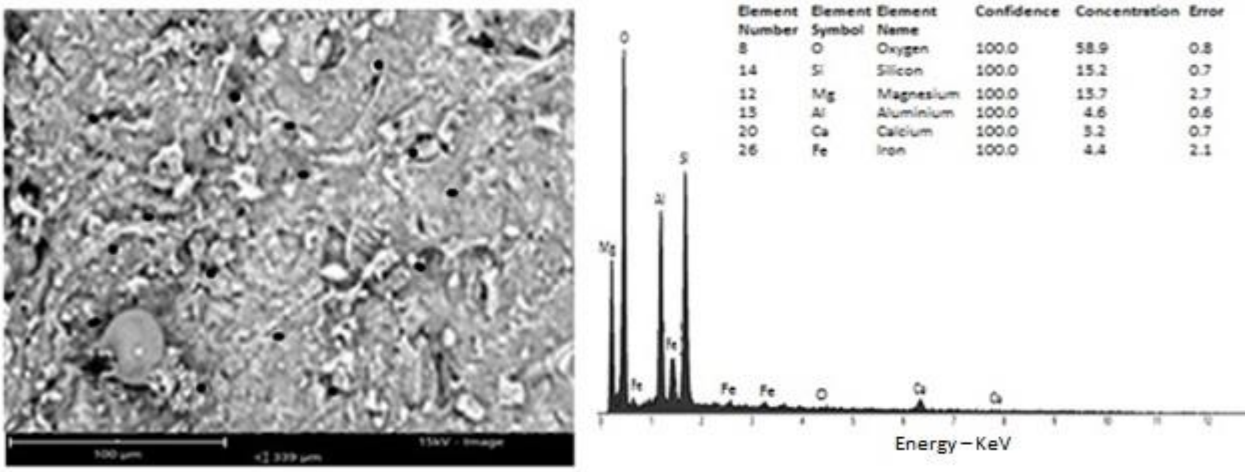

Element Number	Element Symbol	Element Name	Confidence	Concentration	Error
8	O	Oxygen	100.0	58.9	0.8
14	Si	Silicon	100.0	15.2	0.7
12	Mg	Magnesium	100.0	13.7	2.7
13	Al	Aluminium	100.0	4.6	0.6
20	Ca	Calcium	100.0	3.2	0.7
26	Fe	Iron	100.0	4.4	2.1

Figure 5. Micrograph and EDS spectrum of composite sample C.

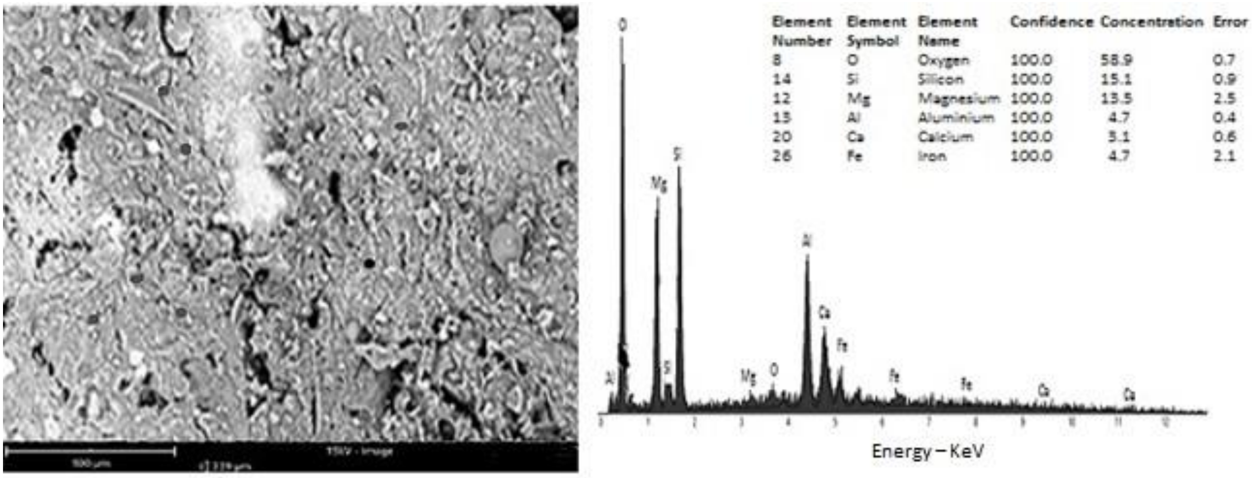

Element Number	Element Symbol	Element Name	Confidence	Concentration	Error
8	O	Oxygen	100.0	58.9	0.7
14	Si	Silicon	100.0	15.1	0.9
12	Mg	Magnesium	100.0	13.5	2.5
13	Al	Aluminium	100.0	4.7	0.4
20	Ca	Calcium	100.0	3.1	0.6
26	Fe	Iron	100.0	4.7	2.1

Figure 6. Micrograph and EDS spectrum of composite sample D.

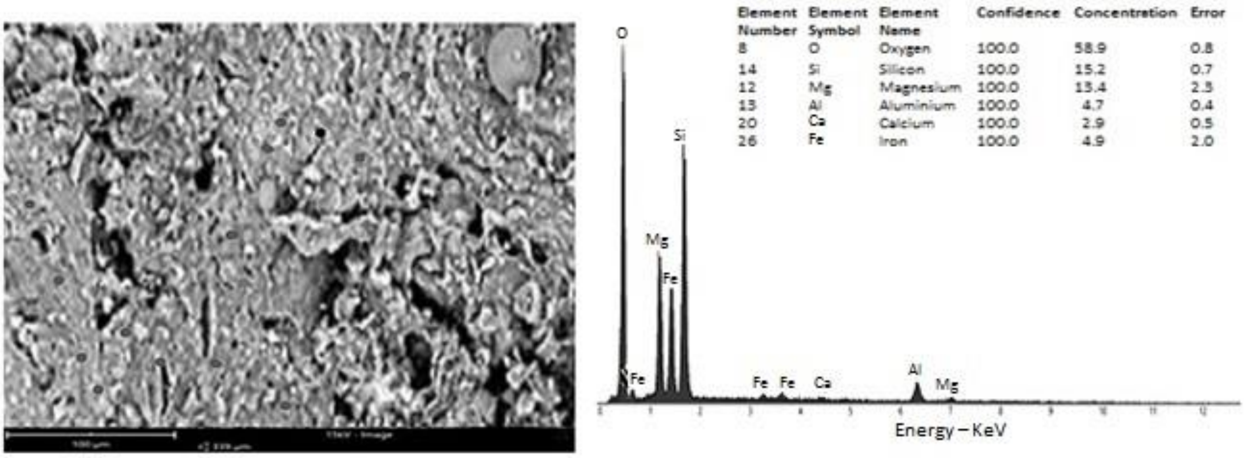

Element Number	Element Symbol	Element Name	Confidence	Concentration	Error
8	O	Oxygen	100.0	58.9	0.8
14	Si	Silicon	100.0	15.2	0.7
12	Mg	Magnesium	100.0	13.4	2.3
13	Al	Aluminium	100.0	4.7	0.4
20	Ca	Calcium	100.0	2.9	0.5
26	Fe	Iron	100.0	4.9	2.0

Figure 7. Micrograph and EDS spectrum of composite sample E.

3.2. Density of the Composites

There was a gradual increase in the density of the composites from 1.71 to 1.92 g/cm^3 as illustrated in Figure 8. It was observed that the samples exhibited higher density as the concentration of iron millscale increased in the formulation (Table 2).

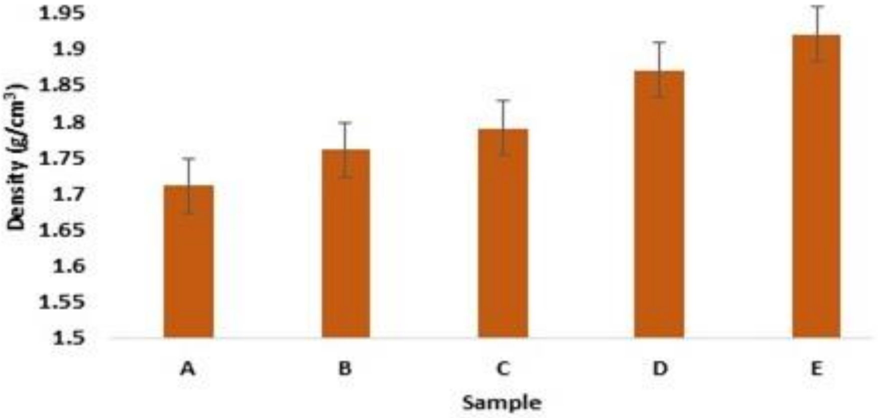

Figure 8. Density of the composite samples.

This characteristic was aided by effective bonding of iron millscale particles during sintering with the particles of other ceramic materials which caused strong interfacial bonding. This corroborated the maxim that iron based friction materials retain some particular properties among which is high density [14]. The increase in density was also due to the deposition of iron as a result of diffusion into the ceramic phase which agreed well with the result of iron infiltration in ceramics as reported during In-situ TiC-Fe-Al_2O_3-TiAl/Ti_3Al composite coating processing using centrifugal assisted combustion synthesis [15]. Conventional automobile brake pad has density of 1.89 g/cm^3 [4] while the density range of the samples is 1.71 to 1.92 g/cm^3 which is an indication that the density of the samples compares very well with that of the conventional brake pad.

3.3. Water Absorption

The water absorption behaviour of the composites during immersion in water for a period of two days is illustrated in Figure 9. Water absorption could be detrimental to the physical and mechanical properties of materials [13]. Sample A exhibited the highest level of water absorption of 0.4 % while other samples exhibited water absorption level of 0.3 %. This is an indication of the presence of pores/voids in the microstructure that have been occupied by water [16]. This is also similar to the earlier report of [17].

The range of water absorption exhibited by the composites is 0.3 – 0.4 % which is very low. The reason for the reduced water absorption capacity could be due to the adhesion of particles which led to decrease in porosity level [4]. The sintering of the materials at elevated temperature during production enhanced the bonding of the materials. The results obtained in this study compared favourably with water absorption level of conventional brake pad which is 0.9 % [4].

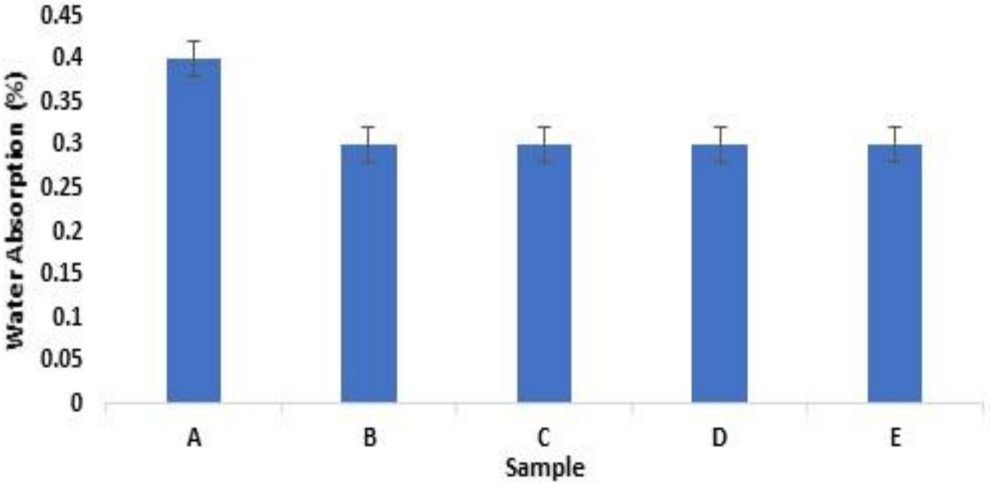

Figure 9. Water absorption of the composite samples

3.4. Hardness of the Composites

The hardness of materials implies resistance to indentation, permanent or plastic deformation. From the results shown in Figure 10, the hardness values of the samples are high. This is attributable to the presence of silica (SiO_2), magnesia (MgO), alumina (Al_2O_3), FeO, Fe_2O_3, and CaO as shown by the X-ray fluorescence analysis (Table 1). These are hard materials [18, 19]

.

The hardness value of sample A (control) which was not blended with iron millscale is 131.13 BHN while the other samples that were blended with iron millscale exhibited higher hardness than sample A. Sample D that was blended with 12 wt. % of iron millscale exhibited the highest hardness value of 147.09 BHN. This indicates the ability of the blend of particles of the composites in enhancing the hardness of the composites. The uniform dispersion of the particles as observed in the microstructure and strong bonding/adhesion of particles must have also contributed to the enhancement of the hardness. The reduction observed in hardness beyond 12 wt.% of millscale addition may be due to improper dispersion of the filler in the matrix resulting to weak adhesion of particles. This is similar to the earlier report/postulation of [20].

The hardness value of automobiles commercial brake pad is 101 BHN [5]. The range of the hardness of the composites is 131.13 – 147.09 BHN. Sample D exhibited the highest hardness value of 147.09 BHN which is 31 % higher than that of the conventional automobiles brake pad. This shows that the composite has the potential will perform well in service when used as brake pad. The results have also attested to the fact that ceramic materials usually exhibit very high hardness and compressive strength [21].

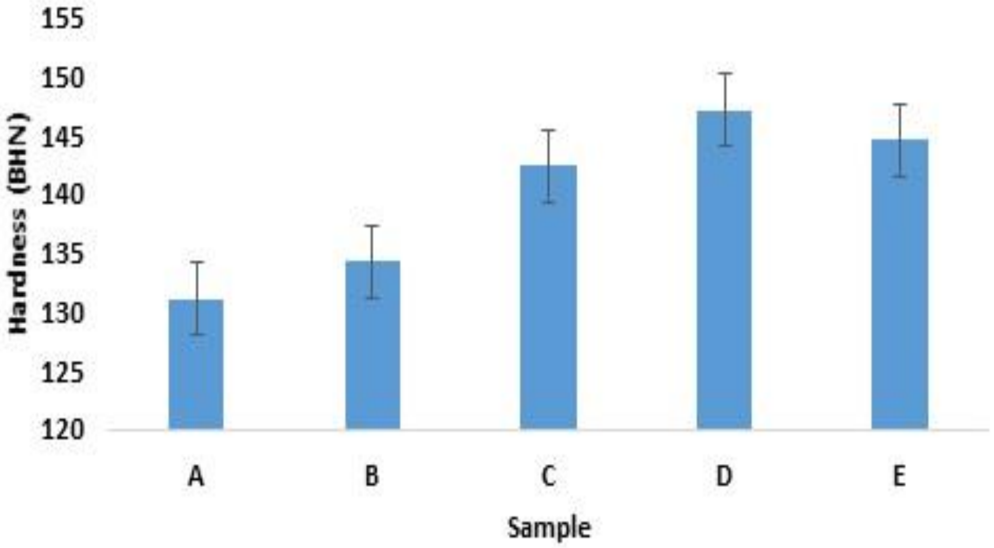

Figure 10. Hardness of the composites

3.5. Compressive Strength of the Composites

There was a gradual increase in the compressive strength of the composites from samples A – D as illustrated in Figure 11. The compressive strength value of sample A (control) which was not blended with iron millscale is 141.16 MPa while the other samples that were blended with iron millscale exhibited higher compressive strength than sample A. Sample D that was blended with 12 wt. % of iron millscale exhibited the highest compressive strength value of 156.45 MPa. The good distribution of the millscale as observed in the microstructure and strong adhesion (bonding) of the particles must have led to the improvement in the compressive strength and also enhanced the composite samples' to prevent gross deformation. This is in agreement with the earlier report of Olabisi et al. [4].

It has been established by Randelovic et al. [22] that strong adhesion interfacial bonding improved the mechanical properties of composites. There was a decrease in the compressive strength of the composite sample E having more than 12 wt. % millscale addition. This could be as a result of weak adhesion of the particles of the materials.

The average compressive strength of conventional automobiles brake pad is 110.07 MPa. The recommended range for brake materials is 70 – 125 MPa [5] while the range of compressive strength of composites obtained in this study is 141.16 – 156.45 MPa. The compressive strength of sample D is greater than that of conventional automobiles brake pad by 25 % which shows that the developed composites have the potential to perform well in service if used as brake pad.

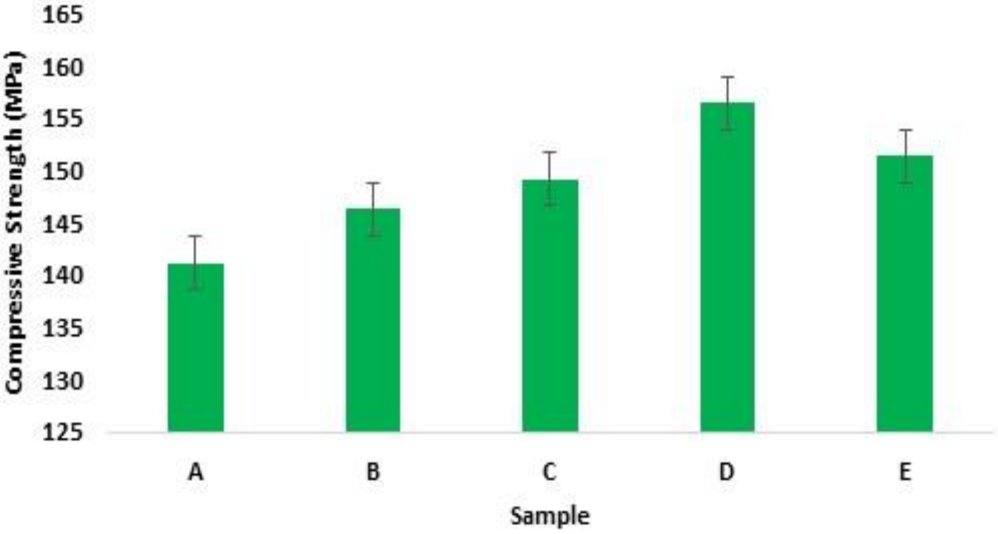

Figure 11. Compressive strength of the composites.

3.6. Shear Strength of the Composites

There was a slight progressive increase in the shear strength of the composites from samples A – D as illustrated in Figure 12. Sample D exhibited the highest shear strength value of 5.97 MPa. The good distribution of the particles in the microstructure as illustrated in Figures 4 – 7 and their adhesion must have been responsible for enhancement of the shear strength of the samples. This agreed with the postulation that strong interfacial bonding between the filler and matrix increases the shear strength [9, 22]. Weak interfacial bonding of the particles could be responsible for the decrease in the shear strength exhibited by sample E having more than 12 wt. % millscale addition.

Conventional automobiles brake pad has shear strength value of 5.46 MPa [5]. The range of shear strength of the composites obtained in this study is 4.82 – 5.97 MPa. This is within the recommended value which is an indication that the developed composites have the potential of performing well in service if used as brake pads.

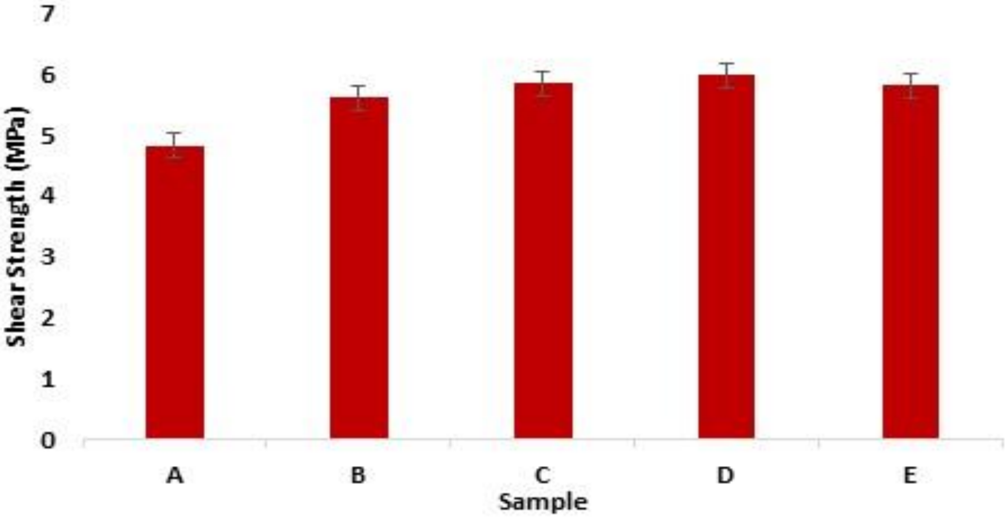

Figure 12. Shear strength of the composites

3.7. Composites' Impact Energy

Energy absorbed by a material before fracture when subjected to rapid (impact) loading is its impact energy. As illustrated in Figure 13, there was a decrease in the impact energy of the samples from A - E. Sample A exhibited the highest impact energy (IE) of 8.03 J while IE of the composites with millscale addition decreased from samples B – E. The decrease in IE may be attributable to the hardness of the materials which imparted brittleness to the composites.

During impact loading, the formation and propagation of cracks and micro-voids [23] within the composites led to the reduction in the impact energy.

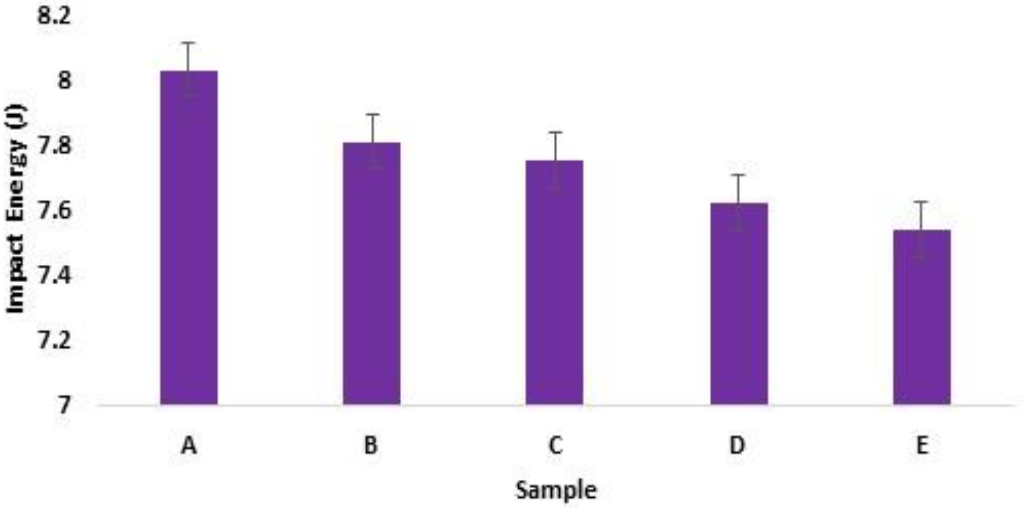

Figure 13. Impact energy of the composites

4. CONCLUSION

In this study, particulate ceramic matrix composites (PCMCs) have been developed via powder metallurgy method. The physical and mechanical properties of the composites were investigated. The ceramic composites exhibited very good properties in terms of density, water absorption, hardness, compressive strength, shear strength, and impact energy. The specific values of these properties exhibited by sample D in terms of density (1.87 g/cm^3), water absorption (0.3 %), hardness (147.09 BHN), compressive strength (156.45 MPa), shear strength (5.97 MPa) and impact energy (7.62 J) are desirable. These results compared favourably well with that of conventional automobiles brake pads which is an indication that the composites are very suitable for application as automobiles brake pads.

ACKNOWLEDGEMENTS

The authors are thankful to the management of the University of Lagos for the research grant (CRC No. 2019/04) provided to carry out this study through the Central Research Committee (CRC).

REFERENCES

[1] Dagwa IM, Ibhadode AO. Some physical and mechanical properties of asbestos free experimental brake pad. Journal of Raw Materials Research (Jormar) 2006; 3(2): 94-103.

[2] Onyeneke FN, Anaele JU, Ugwuegbu CC. Production of motor vehicle brake pad using local materials (periwinkle and coconut shell). International Journal of Engineering and Science (IJES) 2014; 3(9): 17-24.

[3] Nuhu AA, Olabisi AI. Development and evaluation of maize husks (asbestos-free) based brake pad. International Institute for Science, Technology and Education (IISTE): Industrial Engineering Letters-IEL 2015; 5(2): 67 – 80.

[4] Olabisi AI, Ademoh NA, Okechukwu OM. Development and assessment of composite brake pad using pulverized cocoa beans shells filler. International Journal of Materials Science and Applications 2016; 5(2): 66-78.

[5] Dagwa IM, Ibhadode AO. Determination of optimum manufacturing conditions for asbestos-free brake pad using taguchi method. Nigerian Journal of Engineering Research and Development 2006; 5(4): 1–8.

[6] Joseph AB. Enhancement of the nutritive value of cocoa (theobroma cacao) bean shells for use as feed for animals through a two-stage solid state fermentation with pleurotus ostreatus and aspergillus niger. In 2012 Kumasi College of Science, Department of Biochemistry and Biotechnology, Kwame Nkrumah University of Science and Technology.

[7] Okoroigwe EC, Christopher SM, Pascal KD. Characterization of palm kernel shell for materials reinforcement and water treatment. Journal of Chemical Engineering and Materials Science 2014; 5(1): 1-6.

[8] Fagbemigun TK, Fagbemi OD, Otitoju O, Mgbachiuzor E, Igwe CC. Pulp and paper-making potential of corn husk. International Journal of AgriScience 2014; 4(4): 209-213.

[9] Chan D, Stachowiak GW. Review of automotive brake friction materials. Journal of Automobile Engineering, Proceedings of the Institution of Mechanical Engineers 2004; Part D 218(9): 953-966.

[10] Nagesh SN, Siddaraju C, Prakash SV, Ramesh MR. Characterisation of brake pads by variation in composition of friction materials. Elsevier, Procedia Materials Science 2014; 5: 295-302.

[11] Aigbodion VS, Agunsoye JO, Kalu V, Asuke F, Ola S. Microstructure and mechanical properties of ceramic composites. Journal of Minerals & Materials Characterization & Engineering 2010; 9(6): 527-538.

[12] Islam MR, Beg MDH, Gupta A. Characterization of laccase-treated kenaf fibre reinforced recycled polypropylene composite. Bio-resources 2013; 8(3): 3753-3770.

[13] Mat-Shayuti MS, Abdullah MZ. Megat-Yusoff PSM. Water absorption properties and morphology of polypropylene/polycarbonate/polypropylene-graft-maleic anhydride blends. Asian Journal of Scientific Research 2013; 6(2): 167-176.

[14] Asif M, Chandra K, Misra PS. Development of ıron based brake friction materials by hot preform forging technique used for medium to heavy duty applications. Journal of Minerals and Materials Characterisation and Engineering 2011; 10(3): 231-244.

[15] Mahmoodian R, Hassan MA, Hamdi M, Yahya R, Rahbari RG. In-situ TiC-Fe-Al_2O_3-TiAl/Ti_3Al composite coating processing using centrifugal assisted combustion synthesis. Elsevier, Composites Part B: Engineering 2014; 59: 279-284.

[16] Pantyukhov P, Kolesnikova N, Anatoly P. Preparation, structure, and properties of biocomposites based on low-density polyethylene and lignocellulosic fillers. Polymer Composites 2016; 37: 1461–1472.

[17] Tewari M, Singh VK, Gope PC, Chaudhary AK. Evaluation of mechanical properties of bagasse-glass fiber reinforced composite. Journal of Materials and Environmental Science 2012; 3(1): 171-184.

[18] Hassan SB, Aigbodion VS. Microstructure and interfacial reaction of Al-Cu-Mg/bagasse ash particulate composite. Journal of Alloy & Compounds 2010; 491: 571–574.

[19] Aku SY, Yawas DS, Madakson PB, Amaren SG. Characterisation of periwinkle shell as asbestos-free brake pad materials. Pacific Journal of Science and Technology 2012; 13(2): 57-63.

[20] Agunsoye JO, Talabi SI, Awe O, Kelechi H. Mechanical properties and tribological behaviour of recycled polyethylene/cow bone particulate composite. Journal of Materials Science Research 2013; 2: 41-50.

[21] Callister WD, Balasubramaniam R. Materials Science and Engineering. In 2011 7th Edition, Wiley India Pvt. Ltd., 4435-36/7, New Delhi-110002, India, ISBN 978-81-265-2143-2.

[22] Randelovic MS, Zarubica AR, Purenovic MM. New Composite Materials in the Technology for Drinking Water Purification from Ionic and Colloidal Pollutants. In 2012 Online [Available]: http://dx.doi.org/10.5772/48390pdf. Accessed on October 20, 2017.

[23] Manikandan A, Rajkumar R. Evaluation of mechanical properties of synthetic fiber reinforced polymer composites by mixture design analysis. Polymers & Polymer Composites 2016; 24(7): 455-462.